



INFLUENCE OF INFILL AND NOZZLE DIAMETER ON POROSITY OF PLA 3D PRINTED PARTS

Nor Aiman Sukindar^{1,3}, Ahmad Shah Hizam Md Yasir², Shafie Kamaruddin³, Muhammad Afiq Iman Mohd Nazli³, Mohamad Talhah Al Hafiz Mohd Khata³, Ahmad Azlan Ab Aziz⁴, Ahmad Syamaizar Haji Ahmad Sabli¹, Muhammad Mukhtar Noor Awalludin³, Mohamad Nor Hafiz Jamil³

¹ School of Design, Universiti Teknologi Brunei, Tungku Highway, Gadong BE1410, Brunei Darussalam

² Faculty of Resilience Rabdan Academy, 65, Al Inshirah, Al Sa'adah, Abu Dhabi, 22401,

PO Box: 114646, Abu Dhabi, UAE

³ Manufacturing and Materials Department, International Islamic University Malaysia, 53100 Gombak, Selangor, Malaysia

⁴ Faculty of Engineering, Universiti Teknologi Brunei, Tungku Highway, Gadong BE1410, Brunei Darussalam

Corresponding author: Nor Aiman Sukindar, noraimansukindar@gmail.com

Abstract: This study investigates the influence of infill density, infill pattern, and nozzle diameter on the porosity of polylactic acid (PLA) parts fabricated using fused filament fabrication (FFF). Nine different parameter combinations were evaluated using a Taguchi L9 orthogonal array, involving three infill densities (15%, 45%, 75%), three nozzle diameters (0.2 mm, 0.4 mm, 0.6 mm), and three infill patterns (grid, cubic, gyroid). Porosity was measured using gravimetric methods and supported by Scanning Electron Microscopy (SEM). Results showed that infill density was the most significant factor, reducing porosity from 84.98% at 15% to 28.78% at 75% ($p = 0.000$). Nozzle diameter also affected porosity, decreasing from 58.17% at 0.2 mm to 55.61% at 0.6 mm ($p = 0.062$). The influence of infill pattern, while not statistically significant ($p = 0.093$), was visually evident: the grid pattern consistently resulted in lower porosity (~56.22%) due to uniform filament paths, while the gyroid pattern exhibited the highest porosity (~58.45%) due to its complex, non-intersecting structure. The optimal combination for minimizing porosity included a 75% infill density, grid pattern, and 0.6 mm nozzle diameter. These findings provide valuable guidelines for optimizing FFF parameters to improve the structural quality of PLA printed components.

Keywords: infill density; infill pattern; nozzle diameter; porosity; polylactic acid

1. INTRODUCTION

Additive manufacturing (AM), commonly referred to as 3D printing, is an innovative technologies that constructs physical objects layer by layer from digital CAD models. Unlike subtractive manufacturing, which removes material to form a product, AM enables the creation of complex geometries, reduces waste, and accelerates production timelines. Among the various AM technologies, such as Stereolithography (SLA), Selective Laser Sintering (SLS), and Binder Jetting, Fused Filament Fabrication (FFF) is considered the most accessible due to its simplicity, affordability, and compatibility with numerous thermoplastic materials [1]. As a result, FFF is widely employed in automotive, healthcare, education, and consumer industries where rapid prototyping and functional part production are essential [2]. Despite its many advantages, FFF is subject to certain manufacturing defects, with porosity being one of the most significant concerns. Porosity refers to the formation of internal voids or air pockets that result from inadequate inter-layer bonding, uneven extrusion, or improper cooling during the printing process [3]. These voids function as stress concentrators and reduce the overall strength, dimensional accuracy, fatigue life, and environmental resistance of printed components. The occurrence of porosity is not evenly distributed throughout a printed object. Regions such as outer perimeters and the top and bottom layers often receive multiple extrusion passes at near-100% density, resulting in fewer voids and more precise dimensions. In contrast, internal infill regions especially those printed at low densities are more susceptible to void formation due to reduced material overlap and bonding [4].

Among the various print parameters, infill density plays a critical role in influencing porosity and mechanical performance. A higher infill density increases the amount of material within a part, which enhances bonding between extruded lines and reduces the occurrence of internal voids [5]. Several studies have demonstrated that

increasing infill density from 25% to 75% can significantly improve tensile and compressive strength because of the decreased void volume [3]. However, very low infill densities, while beneficial for reducing material use and shortening print time, can result in structural discontinuities that weaken the part under mechanical load, especially during cyclic or dynamic applications [6]. Nozzle diameter is another essential factor affecting the structural quality of FFF parts. Larger nozzle diameters, such as 0.6 mm, allow for wider filament extrusion, which promotes stronger bonding between layers and reduces the likelihood of porosity formation [7]. On the other hand, smaller nozzles, such as 0.2–0.4 mm, provide finer detail and higher surface resolution. However, these smaller diameters can lead to under-extrusion, uneven material flow, and poor layer adhesion if not properly controlled, thereby increasing porosity [8]. These problems are often aggravated under conditions of rapid printing speeds or suboptimal extrusion temperatures [9].

The infill pattern, or the internal geometric structure used to fill the part, also significantly influences the part's strength and porosity. Common patterns such as grid and rectilinear offer consistent overlap and stress distribution, resulting in fewer internal voids [10]. In contrast, more complex patterns such as honeycomb, gyroid, and cubic structures are designed for material efficiency and energy absorption but tend to produce irregular voids at junctions and curved paths due to inconsistent filament contact [11,6,12]. Therefore, selecting the appropriate infill pattern must take into account the mechanical requirements and intended function of the printed component. It is worth noting that the choice of infill pattern not only affects structural behavior but also impacts thermal conductivity and energy dissipation during part usage [13]. Furthermore, porosity is often region-specific within a printed part. The outer walls and top/bottom surfaces usually exhibit low porosity because they are printed with solid or nearly solid material layers. These areas benefit from high extrusion density and greater pressure during deposition, leading to superior dimensional stability and minimal internal voids [4]. In contrast, the interior infill, particularly at low densities, exhibits higher porosity due to reduced overlap and weaker inter-layer contact. These microstructural inconsistencies are frequently analyzed using Scanning Electron Microscopy (SEM) or X-ray Computed Tomography (CT), which provide detailed visualization and quantification of void distribution within the part [2,4]. It is important to recognize that the quality of FFF parts is not solely determined by individual parameters. Instead, the interaction among various settings, including nozzle diameter, infill density, and infill pattern, collectively dictates the structural performance and porosity characteristics. Researchers have employed statistical tools such as Taguchi designs, analysis of variance (ANOVA), and regression modeling to evaluate how these parameters interact with one another [14]. For instance, the effect of nozzle diameter on bonding and porosity can be amplified or mitigated depending on the chosen infill pattern and print speed [15,16]. Moreover, optimizing these parameter combinations can enhance not only mechanical strength but also material efficiency and printing speed [12]. Although a considerable number of studies have investigated the effects of individual printing parameters, there is a lack of comprehensive research that explores their combined and region-specific impacts on porosity. Recent developments in numerical modeling, particularly Finite Element Analysis (FEA), have made it possible to simulate deformation behavior and void formation within complex geometries. These simulations, when validated with experimental data, offer valuable insight into process optimization for FFF printing [17]. Furthermore, novel approaches such as sinusoidal or gradient extrusion paths are being developed to reduce internal voids and improve strength anisotropy by gradually varying material density across regions [18]. For these reasons, the present study aims to systematically investigate the combined effects of infill density, nozzle diameter, and infill pattern on both global and region-specific porosity to porosity of printed parts.

2. MATERIALS AND METHODS

2.1. Materials and Equipment

In this study, polylactic acid (PLA) filament was used as the base printing material. Specifically, eSUN PLA Lite was selected due to its high dimensional stability and biodegradability. The filament has a nominal diameter of 1.75 mm and a manufacturer-specified density of 1.23 g/cm³. All parts were printed using a Bambu Lab A1 Mini desktop FFF 3D printer. The printer is equipped with an automatic bed leveling system, a direct-drive extruder, and allows precise control over nozzle diameter and print speed. Slicing and G-code generation were performed using Bambu Studio software.

2.2. Sample Design

All samples were modeled using SolidWorks CAD software and exported in STL format. The design consisted of a box-shaped object with dimensions of 20 mm × 20 mm × 20 mm. A total of nine different parameter sets were created, combining three infill densities (15%, 45%, and 75%), three nozzle diameters (0.2 mm, 0.4 mm, and 0.6 mm), and three infill patterns (grid, cubic, and gyroid). These combinations were generated using Taguchi method via Minitab software for efficient design of experiments.

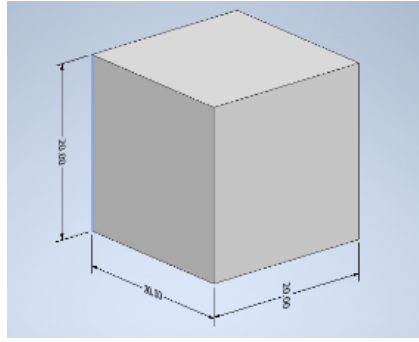


Fig. 1. 3D design of the sample

2.3. Porosity Calculus

The porosity of the printed part then needs to be calculated by using formula. The initial formula to calculate the porosity of the printed parts is from Equation 1. The material volume was determined by using Equation 2 which utilises the density value of the PLA-lite. The theoretical density of the PLA-lite was stated to be 1.23 g/cm³.

$$\text{Porosity (\%)} = (\text{Total Volume} - \text{Material volume} / \text{Total volume}) \times 100 \quad (1)$$

$$\text{Material volume} = \text{Mass} / \text{Density} \quad (2)$$

Next, from the Equation 2, the mass of the printed parts needs to be measured. The equipment that is suitable to be used is analytical balance which is extremely accurate laboratory balance. The balance offers a readability up to 0.00001 grams (0.01 mg) which can measure the printed parts accurately. The length, width and height of the samples were measured using vernier calliper.

2.3. Microstructure Observation

Scanning Electron Microscopy (SEM) was used to observe the internal microstructure of the printed parts. Scanning Electron Microscopy (SEM) analysis was conducted using an InTouchScope JSM-IT100 series SEM (JEOL Ltd., Japan) Samples representing low (15%) and high (75%) infill densities, as well as samples with varying nozzle diameters, were selected. SEM imaging was conducted at 30× magnification to capture surface features and internal voids. This qualitative analysis enabled visualization of pore distribution, inter-layer bonding, and surface topology, supporting the quantitative porosity results.

2.4. Experimental Design

The design of the experiment in the study used to systematically investigate the effects of 3D printing parameters which are, the infill density (15%, 45% and 75%), the infill pattern (grid, cubic and gyroid) and the nozzle diameter (0.2mm, 0.4mm and 0.6mm) on the porosity of the printed parts. Taguchi method was utilized in this study by using Minitab software. Table 1 shows the various set combinations of parameters that will be printed.

Table 1. Set of runs from Minitab software

Samples	Infill Density (%)	Nozzle Diameter (mm)	Infill Pattern
1	15	0.2	Grid
2	15	0.4	Cubic
3	15	0.6	Gyroid
4	45	0.4	Grid
5	45	0.6	Cubic
6	45	0.2	Gyroid
7	75	0.6	Grid
8	75	0.2	Cubic
9	75	0.4	Gyroid

3. RESULTS AND DISCUSSION

This chapter presents the results and analysis of the study, structured to align with the research objectives. It begins with a detailed discussion of the data collected, followed by an in-depth interpretation of the findings. The results included the measurement of the dimensional accuracy of the printed samples, its porosity and the justification image from Scanning Electron Microscopy (SEM). Figure 2 shows all nine printed samples.

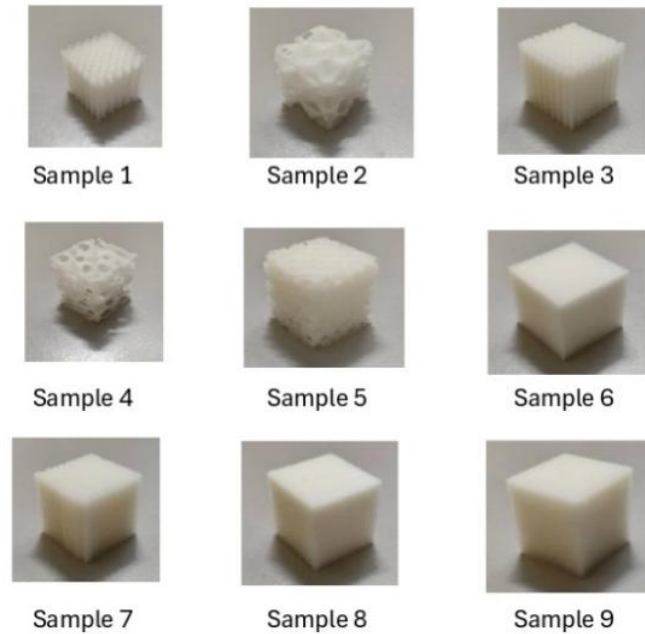


Fig. 2. Printed samples

3.1. Result of the porosity measurement

Table 2 presents the dimensional measurements of the printed samples, recorded using a calibrated vernier caliper. Accurate measurement of the length, width, and height for each sample was essential in calculating the total volume, which was later used to determine the porosity percentage. Consistent dimensions across replicates helped ensure that volume-based porosity calculations remained reliable and valid for comparison.

Table 2. Sample Measurement

Samples	Dimension (mm)		
	Length	Width	Height
1	20.10	20.00	20.00
	20.06	20.02	20.00
	20.08	20.04	19.98
2	20.12	20.02	20.08
	20.06	20.00	20.08
	20.08	20.00	20.06
3	20.10	20.16	20.28
	20.10	20.08	20.28
	20.12	20.10	20.20
4	20.12	20.02	20.06
	20.10	20.00	20.06
	20.08	20.04	20.08
5	20.20	20.20	20.22
	20.16	20.20	20.18
	20.18	20.12	20.18
6	20.04	19.98	19.98
	20.02	20.00	20.00
	20.00	20.02	20.04

7	20.28	20.28	19.98
	20.22	20.26	20.00
	20.26	20.24	20.02
8	20.36	20.10	20.32
	20.30	20.22	20.20
	20.28	20.20	20.22
9	20.06	20.02	19.88
	20.08	20.04	20.00
	20.06	20.02	20.00

Table 3 summarizes the mass, calculated material volume, and average porosity for each sample. The weight of each sample was measured using a precision digital scale, and the material volume was calculated using the known density of PLA (1.23 g/cm³). The porosity was then derived by comparing the theoretical volume (based on geometric dimensions) and the actual material volume, as calculated from the mass.

Table 3. Average porosity measurement for each sample

Samples	Weight (g)	Material volume=weight/density	Average Porosity (%)
1	1.4734	1197.8861	84.98
	1.4962	1216.4228	
	1.4853	1207.5610	
2	1.6470	1339.0244	83.86
	1.6106	1309.4309	
	1.5471	1257.8049	
3	1.7219	1399.9187	82.87
	1.7270	1404.0650	
	1.7279	1404.7967	
4	4.4874	3648.2927	54.91
	4.4964	3655.6098	
	4.4507	3618.4553	
5	4.5468	3695.5854	55.17
	4.5228	3677.0732	
	4.5310	3683.7398	
6	3.9749	3231.6260	59.67
	3.9789	3234.8780	
	3.9661	3224.4715	
7	7.1664	5826.3415	28.78
	7.1983	5852.2764	
	7.1670	5826.8293	
8	7.1500	5813.0081	29.87
	7.1649	5825.1220	
	7.1574	5819.0244	
9	6.6017	5367.2358	32.80
	6.6500	5406.5041	
	6.6360	5395.1220	

A clear trend is observed across the samples: porosity decreases significantly as infill density increases, confirming the strong relationship between material deposition and internal void content. Samples 1, 2, and 3, all associated with the lowest infill density have exhibited the highest porosity values, measuring 84.98%, 83.86%, and 82.87%, respectively. These high porosity percentages indicate a substantial presence of air gaps and poor internal consolidation, typical of sparse infill patterns where large volumes remain unfilled. In contrast, Samples 7, 8, and 9, all printed at high infill densities and with larger nozzle diameters, demonstrated the lowest porosity values, measuring 28.78%, 29.87%, and 32.80%, respectively. The reduced porosity in these samples reflects a

denser and more compact internal structure with improved inter-layer and intra-layer fusion. These results align with the findings of Brackett et al. and Müller et al., who reported that increasing infill percentage significantly reduces porosity and enhances mechanical strength in FFF-printed PLA parts [3,5]. Samples 4, 5, and 6 demonstrated intermediate porosity values, averaging 54.91%, 55.17%, and 59.67%, respectively. These results reflect moderate material fill, where partial fusion and moderate overlap between filaments result in an internal structure that is neither sparse nor fully dense. These values are useful benchmarks for applications requiring a balance between structural strength and weight savings. Fig 3 visually summarizes the average porosity values for all samples, illustrating the variation in porosity resulting from different parameter combinations. The graph clearly highlights the inverse relationship between infill density and porosity, as well as the combined effects of nozzle diameter and infill pattern on material distribution. The results show the importance of selecting optimal printing parameters based on the desired structural density and performance of the final part. Overall, this analysis demonstrates that porosity in FFF-printed PLA components is highly sensitive to changes in infill density, nozzle diameter, and infill pattern. The data confirm that higher material deposition and wider extrusion paths are key to reducing void formation and improving print quality, which is consistent with trends reported in prior literature [6,7].

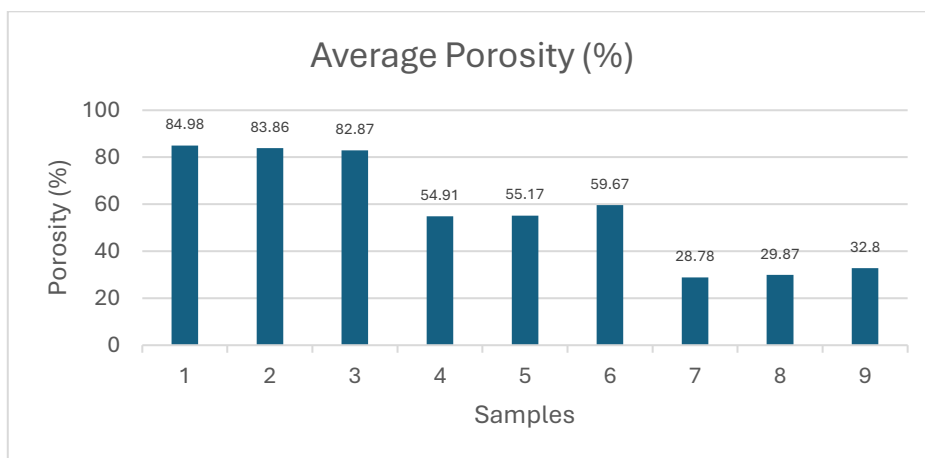


Fig. 3. Average Porosity bar graph

3.2. Optimal Combination of Parameters to Obtain Porosity

Table 4 shows a response table for means that summarize the results from a Taguchi method analysis, highlighting the impact of three factors which are infill density, infill pattern and nozzle diameter. From the table, each parameter is analyzed at three levels, with the mean porosity values calculated for each level.

Table 4. Analysis Variance for All Variables

Level	Infill Density	Infill Pattern	Nozzle Diameter
1	83.90	56.22	58.17
2	56.58	56.30	57.19
3	30.48	58.45	55.61
Delta	53.42	2.22	2.57
Rank	1	3	2

The analysis reveals that infill density exerts the most significant effect on porosity, as indicated by the highest Delta value of 53.42. This result confirms that increasing infill density greatly reduces internal voids by enhancing material distribution and inter-layer bonding, in agreement with findings by [3,5]. Nozzle diameter ranks second in influence, with a Delta of 2.57, suggesting that larger diameters slightly improve material fusion and reduce porosity. Infill pattern, with a Delta of 2.22, shows the least effect among the three parameters, although subtle structural differences are still observed across pattern types.

The regression model is highly significant overall, as indicated by a p-value of < 0.001, with most of the total variance (4297.84 out of 4306.49) being explained by the model. Among the factors, infill density contributes the most to the variance, with statistically significant p-value of < 0.001. This suggests that infill density is the primary factor influencing the porosity. In contrast, infill pattern and nozzle diameter contribute much less to the variance.

While both factors show moderate effects with the p-values of 0.093 and 0.062 indicate that they are not statistically significant at the 0.05 level.

Table 5. Analysis of Porosity with Infill Density, Infill Pattern and Nozzle Diameter

Source	DF	Adj SS	Adj MS	F-Value	P-Value
Regression	3	4297.84	1432.61	828.47	0.000
Infill Density	1	4280.54	4280.54	2475.41	<0.001
Infill Pattern	1	7.41	7.41	4.29	0.093
Nozzle Diameter	1	9.88	9.88	5.71	0.062
Error	5	8.65	1.73		
Total	8	4306.49			

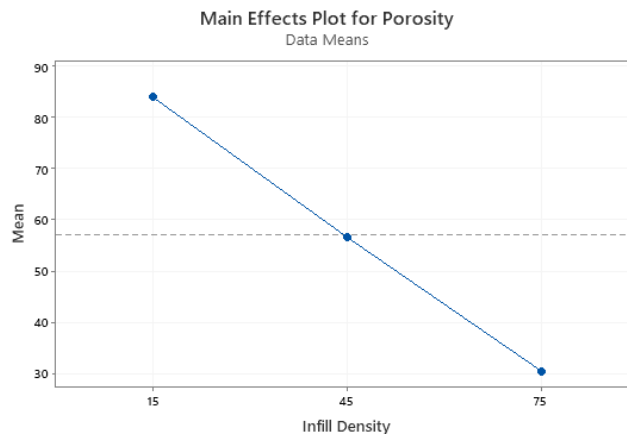


Fig. 4. Graph plot for infill density and porosity

Figure 4 shows the correlation between infill density and resulting porosity in 3D printed parts which providing an insight into how changing the material usage influence internal void spaces. The X-axis of the graph represent the levels of infill density and y-axis shows the corresponding mean porosity values. The Fig. 4 shows a clear and consistent negative correlation between infill density and porosity, indicating that as the infill density increases, the porosity significantly decreases. When the infill density at 15%, the porosity is at its highest. As the infill density increase to 45%, the porosity slightly decreases to around and the porosity is at its lowest when the infill density is at 75% indicating much denser internal structure with minimal voids. The trend is consistent with the expectation showing that increasing the infill density will reduce the amount of empty space in the printing part. This is because increasing the infill density will lead to the increased amount of material deposited within the structure, leaving less room for voids. This trend supports the expectation that more material deposition results in fewer internal voids. This relationship is well-documented in prior literature [5, 6].

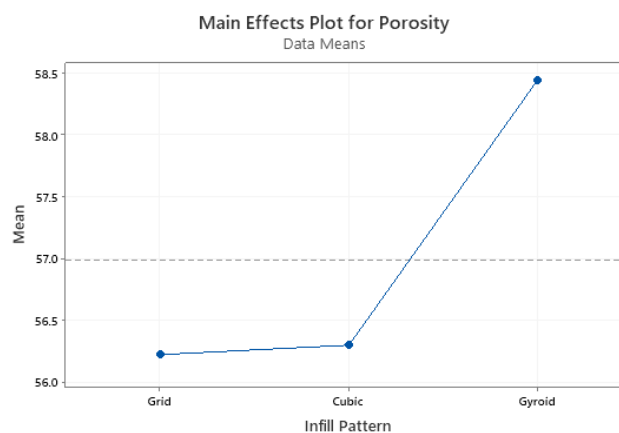


Fig. 5. Graph plot for infill pattern and porosity

Figure 5 displays the correlation between infill pattern and porosity. There are three different infill patterns used which are grid, cubic and gyroid. The grid pattern having lowest mean value, slightly higher for cubic pattern and the gyroid pattern exhibit a significant increase in porosity compared to other two patterns. Even the p-value for

infill pattern is above 0.05, however the graph illustrates that the infill pattern somehow affects the porosity. The variation can be explained by the characteristics of each pattern. Although the ANOVA analysis suggests this parameter is not statistically significant, the graph shows observable trends. The grid pattern, which is composed with a straight, intersecting lines lead to a consistent material overlap and good bonding between layers, resulting to lower porosity. Next, the cubic pattern is a three-dimensional lattice structure and offers good internal structure, however, its complexity may result in a slight gap or incomplete layer bonding, and may introduce minor gaps at node intersections. Lastly, for the gyroid pattern consistently results in higher porosity, likely due to its smooth, curving geometry that limits material overlap and bonding pressure [11,12].

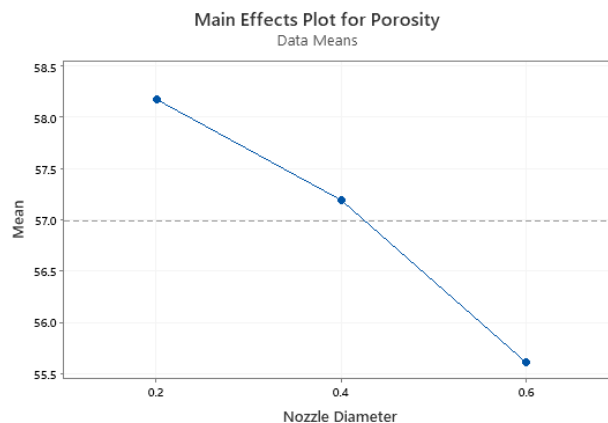


Fig. 6. Graph plot for nozzle diameter and porosity

Figure 6 illustrates the relationship between nozzle diameter and porosity based on data means. The graph shows a decrement gradually for three different nozzle diameters which are 0.2mm, 0.4mm and 0.6mm. From the graph, as the nozzle diameter increases, the porosity decreases, with the highest porosity observed at a 0.2 mm nozzle diameter and the lowest at 0.6 mm. This negative correlation can be explained by the influence of nozzle size on layer thickness and void formation during the 3D printing process. Larger nozzle diameters extrude more material per pass, resulting in thicker layers that improve inter-layer bonding. The larger nozzles create wider extrusion paths, covering more surface area and minimizing gaps within a single layer. This results in fewer voids and more homogeneous internal structures [7]. In contrast, smaller nozzle diameters produce thinner layers that cool quickly, before achieving adequate bonding, which can result in higher void formation. Narrower extrusion paths from smaller nozzles also increase the chance of gaps between lines, contributing to greater porosity [8].

3.3. Scanning Electron Microscopy (SEM)

This section presents the results and analysis of the microstructural investigation of PLA printed parts conducted using Scanning Electron Microscopy (SEM). The primary aim of this analysis is to examine the internal structure and identify variations in porosity at a microscopic level. By observing the microstructure, insights into the distribution, size, and shape of pores are obtained, providing a deeper understanding of how the printing parameters such as infill density, infill pattern, and nozzle diameter affect the overall porosity.

Figures 7 and 8 display SEM micrographs of printed samples with two different infill densities: Sample 1 at 15% (Fig. 7) and Sample 9 at 75% (Fig. 8). Both images were captured at $\times 30$ magnification to allow comparison of internal structure, pore size, and filament deposition patterns. In Fig. 7, the microstructure of the sample printed at 15% infill density clearly reveals large voids and open gaps between adjacent filaments. The material distribution is sparse, and the infill lines are widely spaced with minimal overlap. This results in significant porosity due to the reduced number of interfacial bonding points and insufficient material to occupy the internal volume. The poor filament interconnection increases the likelihood of stress concentration zones and weakens the mechanical performance of the part. These findings are consistent with results reported by Müller et al., who found that lower infill densities lead to a higher presence of internal voids and reduced structural coherence in FFF-printed PLA components [5].

Figure 8 illustrates the microstructure of the sample printed at 75% infill density. A more compact and continuous internal network is observed, with thicker walls and fewer gaps between extruded filaments. The improved material coverage results in stronger bonding between adjacent strands and a substantial reduction in pore volume. This denser structure contributes to higher mechanical strength and dimensional stability, which is especially important for load-bearing applications. Similar conclusions were drawn by Brackett et al., who demonstrated that increasing infill percentage significantly decreases porosity and improves tensile properties in FFF parts [3].

The visual contrast between the two SEM images reinforces the importance of infill density as a dominant factor influencing porosity. As supported by the Taguchi analysis in this study, infill density exhibited the highest Delta value, confirming its primary contribution to porosity variation across the printed samples.

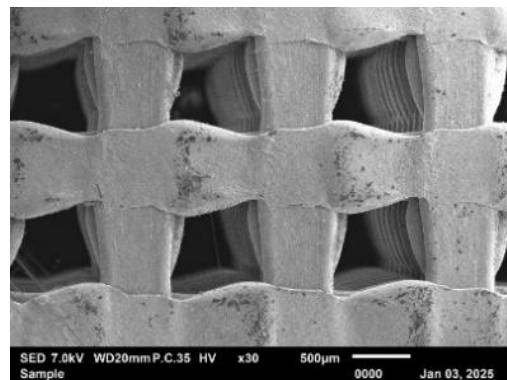
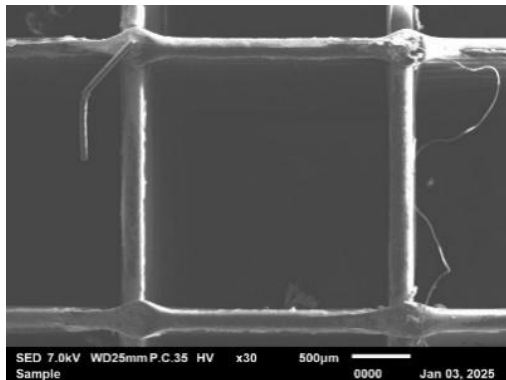


Fig. 7. Microstructure for Sample 1 (15% infill density) Fig. 8. Microstructure for Sample 9 (75% infill density)

Figures 9 and 10 display SEM micrographs comparing the layer structure of parts printed using two different nozzle diameters: 0.2 mm (Sample 6) and 0.6 mm (Sample 7), both at $\times 30$ magnification. These images provide valuable insights into the impact of nozzle size on layer formation, uniformity, and deposition behavior.

In Figure 9, the sample printed with the 0.2 mm nozzle exhibits thinner and more uniform layers, with an average measured thickness of $248.042\ \mu\text{m}$. This finer layer resolution enables more precise geometric detailing and smoother surface finishes, characteristics often sought in high-resolution or intricate part applications. The compact and tightly stacked deposition profile minimizes inter-layer gaps and promotes better fusion, which can potentially enhance dimensional accuracy and reduce macroscopic porosity. However, such precision comes with trade-offs smaller nozzles typically require slower print speeds and are more prone to filament clogging, especially when printing filled or flexible materials. These findings align with those of [8] who reported that while small nozzles improve resolution, they may result in localized micro-voids due to rapid cooling and restricted flow rates.

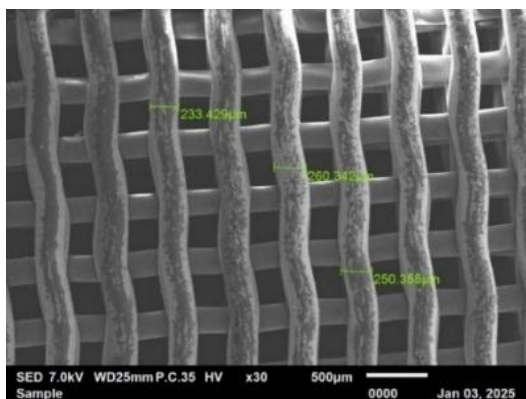


Fig. 9. Measured layer thickness for Sample 6 (0.2 mm nozzle diameter)

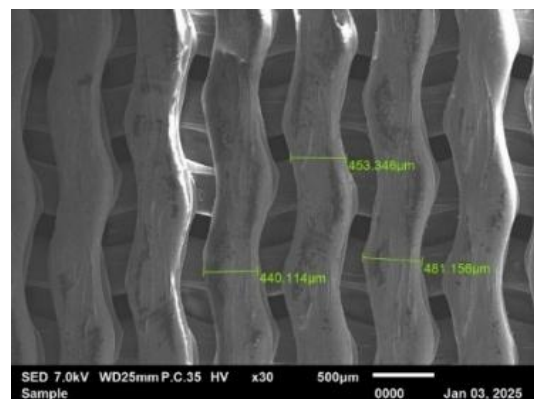


Fig. 10. Measured layer thickness for Sample 7 (0.6 mm nozzle diameter)

In contrast, Fig. 10 shows the microstructure of Sample 7 printed with a 0.6 mm nozzle. The three measured layer thicknesses that are $453.346\ \mu\text{m}$, $481.156\ \mu\text{m}$, and $440.114\ \mu\text{m}$, yield an average of $458.205\ \mu\text{m}$. This significantly thicker deposition allows for faster print times and is advantageous when producing large components or requiring high build rates. However, the increased layer height also introduces more prominent surface undulations and larger inter-layer boundaries. These features can impair mechanical performance due to inconsistent stress distribution and weaker layer bonding. The coarse layering visible in the SEM image supports prior findings that larger nozzle diameters may reduce surface quality and increase porosity in geometrically complex areas [7]. Overall, the SEM comparison highlight the trade-off between print resolution and production efficiency. Smaller nozzles are better suited for high-detail, low-porosity applications, while larger nozzles offer time and material efficiency at the potential cost of dimensional precision and strength.

4. CONCLUSION

This study comprehensively examined how infill density, infill pattern, and nozzle diameter influence porosity in FFF-printed PLA parts. A total of nine different sample configurations were tested, combining these parameters using a Taguchi design of experiments. The results offer several key insights into optimizing printing parameters for improved part quality.

Infill density emerged as the most influential parameter affecting porosity. Samples printed with low infill densities (15%) exhibited the highest porosity values, exceeding 80%, due to larger voids and reduced material deposition. In contrast, increasing the infill density to 75% significantly reduced porosity to under 33%, resulting in denser structures with stronger inter-layer fusion.

Secondly, nozzle diameter also affected porosity, but to a lesser extent. Larger nozzle diameters (0.6 mm) produced thicker extrusions and more stable bonding, leading to lower porosity levels.

Thirdly, although infill pattern was not statistically significant in ANOVA analysis ($p > 0.05$), visual and SEM analysis revealed observable effects. The grid pattern consistently showed lower porosity, attributed to its geometric regularity and strong material overlap. In contrast, the gyroid pattern displayed the highest porosity, likely due to its continuous but less-intersecting architecture, which compromises filament bonding in curved regions.

In summary, the optimal parameter combination for minimizing porosity in PLA FFF printing includes a high infill density (75%), a grid infill pattern, and a larger nozzle diameter (0.6 mm). These conditions promote better material distribution, stronger layer bonding, and lower void content, all of which contribute to superior mechanical performance and reliability.

Author Contributions: Conceptualization: Nor Aiman Sukindar, Ahmad Shah Hizam Md Yasir, Methodology: Ahmad Azlan Ab Aziz, Ahmad Syamaizar Haji Ahmad Sabli, Investigation: Muhammad Afiq Iman Mohd Nazli, Mohamad Talhah Al Hafiz Mohd Khata, Mohamad Nor Hafiz Jamil, Data Curation and Analysis: Muhammad Mukhtar Noor Awalludin, Shafie Kamaruddin, Resources: Nor Aiman Sukindar, Ahmad Shah Hizam Md Yasir, Project Administration: Nor Aiman Sukindar, Supervision: Nor Aiman Sukindar, Validation and Visualization: Ahmad Azlan Ab Aziz, Muhammad Mukhtar Noor Awalludin, Writing – Original Draft: Mohamad Talhah Al Hafiz Mohd Khata, Muhammad Afiq Iman Mohd Nazli, Writing – Review & Editing: Nor Aiman Sukindar, Ahmad Shah Hizam Md Yasir, Funding Acquisition: Nor Aiman Sukindar

Funding: This project was funded under the Internal Grant from Universiti Teknologi Brunei, Reference Number: UTB/GSR/2/2024(2).

Conflicts of Interest: The authors declare no conflict of interest.

Acknowledgements: The authors would like to express their sincere appreciation to the School of Design (Product Design), Graduate Studies & Research (GSR) Office, Universiti Teknologi Brunei, and the Advanced Manufacturing and Technology Research Unit (AMTech), International Islamic University Malaysia, for providing the necessary facilities and support throughout the course of this research.

REFERENCES

1. Kechagias, J. D., Zaoutsos, S. (2024). *Effects of 3D-printing processing parameters on FFF parts' porosity: Outlook and trends*. *Materials and Manufacturing Processes*, 39(2), 804–814. <https://doi.org/10.1080/10426914.2024.2304843>
2. Rusińska, M., Gruber, P., Ziółkowski, G., Łabowska, M., Wilińska, K., Szymczyk-Ziółkowska, P. (2023). *The influence of material extrusion process parameters on the porosity and mechanical properties of PLA products for medical applications*. *Acta of Bioengineering and Biomechanics*, 25(3), 25–41. <https://doi.org/10.37190/abb-02304-2023-01>
3. Brackett, J., Cauthen, D., Condon, J., Smith, T., Gallego, N., Kunc, V., Duty, C. (2022). *The impact of infill percentage and layer height in small-scale material extrusion on porosity and tensile properties*. *Additive Manufacturing*, 58, 103063. <https://doi.org/10.1016/j.addma.2022.103063>
4. Oskolkov, A. A., Kochnev, A. A., Krivoshechekov, S. N., Savitsky, Y. V. (2024). *Real-size reconstruction of porous media using the example of fused filament fabrication 3D-printed rock analogues*. *Journal of Manufacturing and Materials Processing*, 8(3), 104. <https://doi.org/10.3390/jmmp8030104>
5. Müller, M., Jirků, P., Šleger, V., Mishra, R. K., Hromasová, M., Novotný, J. (2022). *Effect of infill*

- density in FDM 3D printing on low-cycle stress of bamboo-filled PLA-based material. *Polymers*, 14(22), 4930. <https://doi.org/10.3390/polym14224930>
6. Köymen Çağar, P. (2024). *Effects of material, infill pattern and infill density on the tensile strength of products produced by fused filament fabrication method*. *Journal of Advances in Manufacturing Engineering*, 5(2), 61–73. <https://doi.org/10.14744/ytu.jame.2024.00008>
7. Triyono, J., Sukanto, H., Saputra, R., Smaradhana, D. (2020). *The effect of nozzle hole diameter of 3D printing on porosity and tensile strength parts using polylactic acid material*. *Open Engineering*, 10(1), 762–768. <https://doi.org/10.1515/eng-2020-0083>
8. Chacón, J. M., Caminero, M. Á., Núñez, P. J., García-Plaza, E., Bécar, J. P. (2021). *Effect of nozzle diameter on mechanical and geometric performance of 3D printed carbon fibre-reinforced composites manufactured by fused filament fabrication*. *Rapid Prototyping Journal*, 27(4), 769–784. <https://doi.org/10.1108/rpj-10-2020-0250>
9. Jain, A., Upadhyay, S., Sahai, A., Sharma, R. S. (2023). *Comparing the flexural and morphological properties of dissimilar FFF-fabricated polymer composites*. *Journal of Thermoplastic Composite Materials*, 37(1), 167–191. <https://doi.org/10.1177/08927057231170790>
10. Khaliq, J., Gurrapu, D. R., Elfakhri, F. (2023). *Effects of infill line multiplier and patterns on mechanical properties of lightweight and resilient hollow section products manufactured using fused filament fabrication*. *Polymers*, 15(12), 2585. <https://doi.org/10.3390/polym15122585>
11. Harpool, T. D., Alarifi, I. M., Alshammari, B. A., Aabid, A., Baig, M., Malik, R. A., Mohamed Sayed, A., Asmatulu, R., El-Bagory, T. M. A. A. (2021). *Evaluation of the infill design on the tensile response of 3D printed polylactic acid polymer*. *Materials*, 14(9), 2195. <https://doi.org/10.3390/ma14092195>
12. Lalegani Dezaki, M., Mohd Ariffin, M. K. A. (2020). *The effects of combined infill patterns on mechanical properties in FDM process*. *Polymers*, 12(12), 2792. <https://doi.org/10.3390/polym12122792>
13. Lopes, L., Reis, D., Paula Junior, A., Almeida, M. (2023). *Influence of 3D microstructure pattern and infill density on the mechanical and thermal properties of PET-G filaments*. *Polymers*, 15(10), 2268. <https://doi.org/10.3390/polym15102268>
14. Zandi, M. D., Jerez-Mesa, R., Lluma-Fuentes, J., Roa, J. (2020). *Experimental analysis of manufacturing parameters' effect on the flexural properties of wood-PLA composite parts built through FFF*. *International Journal of Advanced Manufacturing Technology*, 106, 3985–3998. <https://doi.org/10.1007/s00170-019-04907-4>
15. EisaZadeh, H., Torabi, M. (2024). *Multi-objective optimization of fused deposition modeling (FDM) considering filament length, print time, and mechanical properties*. In *Proceedings of the ASME 2024 International Mechanical Engineering Congress and Exposition (Vol. 2: Advanced Manufacturing, V002T03A001)*. ASME. <https://doi.org/10.1115/IMECE2024-139226>
16. Gonabadi, H., Yadav, A., Bull, S. J. (2020). *The effect of processing parameters on the mechanical characteristics of PLA produced by a 3D FFF printer*. *International Journal of Advanced Manufacturing Technology*, 111, 695–709. <https://doi.org/10.1007/s00170-020-06138-4>
17. Provaggi, E., Capelli, C., Rahmani, B., Burriesci, G., Kalaskar, D. M. (2018). *3D printing assisted finite element analysis for optimising the manufacturing parameters of a lumbar fusion cage*. *Materials & Design*, 163, 107540. <https://doi.org/10.1016/j.matdes.2018.107540>
18. Kilian, D., Holtzhausen, S., Groh, W., Sembdner, P., Czichy, C., Lode, A., Stelzer, R., Gelinsky, M. (2022). *3D extrusion printing of density gradients by variation of sinusoidal printing paths for tissue engineering and beyond*. *Acta Biomaterialia*, 158, 308–323. <https://doi.org/10.1016/j.actbio.2022.12.038>